Comparative Gene Expression Analysis of Somatic Cell Nuclear Transfer-Derived Cloned Pigs with Normal and Abnormal Umbilical Cords 1

Authors: Park, Jong-Yi, Park, Mi-Ryung, Hwang, Kyu-Chan, Chung, Ji-Seok, Bui, Hong-Thuy, et al.

Source: Biology of Reproduction, 84(1) : 189-199

Published By: Society for the Study of Reproduction

URL: https://doi.org/10.1095/biolreprod.110.085779

BIOLOGY OF REPRODUCTION **84,** 189–199 (2011)
Published online before print 22 September 2010.
DOI 10.1095/biolreprod.110.085779

Comparative Gene Expression Analysis of Somatic Cell Nuclear Transfer-Derived Cloned Pigs with Normal and Abnormal Umbilical Cords[1]

Jong-Yi Park,[4] Mi-Ryung Park,[4] Kyu-Chan Hwang,[4] Ji-Seok Chung,[4] Hong-Thuy Bui,[4] Teoan Kim,[5] Seong-Keun Cho,[6] Jae-Hwan Kim,[7] Seongsoo Hwang,[8] Soo-Bong Park,[8] Van Thuan Nguyen,[2,4] and Jin-Hoi Kim[3,4]

Department of Animal Biotechnology,[4] Konkuk University, Seoul, Republic of Korea
Department of Physiology,[5] Catholic University of Daegu School of Medicine, Daegu, South Korea
Department of Animal Science,[6] Pusan National University, Miryang, Gyeongnam, Republic of Korea
Department of Biomedical Sciences,[7] College of Life Science, CHA University, Pochon-si, Gyeonggi-do, Republic of Korea
Animal Biotechnology Division,[8] National Institute of Animal Science, Rural Development Administration, Suwon, Republic of Korea

ABSTRACT

Gene expression profiling of compromised umbilical cords (CUCs) derived from somatic cell nuclear transfer (scNT) clones was performed to determine why scNT-derived clones often exhibit malformed umbilical arteries. Umbilical cord samples were obtained from 65 scNT piglets, and of these, nine displayed a CUC. Microscopic analyses of the scNT clones with CUCs (scNT-CUCs) revealed complete occlusive thrombi that were not detected in the arteries of scNT clones with normal umbilical cords (scNT-Ns). Moreover, whereas the allantoic ducts of the scNT-Ns contained columnar epithelium, the scNT-CUCs lacked this epithelial layer. Compared to scNT-Ns, the scNT-CUCs exhibited severe histological damage, including tissue swelling and vein and arterial damage with complete occlusive thrombi. To investigate functional abnormality, gene expression profiles were created in duplicate using the Platinum Pig 13K oligonucleotide microarray, which contains 13 610 probes of 70 bp in length and is capable of interrogating 13 297 targets with up to one probe per target. Probe sets were selected according to a 2-fold or greater increase or decrease of gene expression in scNT-CUCs compared to scNT-Ns. Most genes expressed in scNT-Ns were also expressed by scNT-CUCs. However, most genes involved in transcriptional regulation, such as *JUN*, *JUNB*, and *FOSL2*, showed a significant decrease in expression in the scNT-CUCs, which may produce a ripple effect capable of altering the transcriptomes of many other cellular processes, including angiogenesis, antioxidation, and apoptosis. The scNT-CUCs with thrombosis showed extensive apoptosis leading to placental insufficiency and related pathology. Considering that the umbilical cord plays a role in the transportation of metabolites to the fetus, placental insufficiency in scNT-CUCs may be caused by an increase in apoptotic protein expression from scNT-derived umbilical cords with hypoplastic arteries, and our results provide evidence that porcine oligonucleotide microarray analysis is a useful tool for screening scNT-derived abnormalities in pigs.

assisted reproductive technology, developmental biology, DNA chip, hypoplastic umbilical artery, pig, placenta, somatic cell nuclear transfer, syncytiotrophoblast, trophoblast, umbilical cord

INTRODUCTION

Despite the advantages of somatic cell nuclear transfer (scNT), this procedure produces normal offspring with a very low efficiency, in part because of a high incidence of fetal death resulting from a variety of complications during pregnancy, including fetal overgrowth and placental malformations [1–5]. In addition, scNT cloning is associated with particularly high levels of phenotypic variability [2, 6–9], with 93% of mice, 64% of cattle, 60% of pigs, and 40% of sheep exhibiting some form of abnormality, including pulmonary hypertension and respiratory distress. Many other researchers, however, have observed that cloned animals are healthy and normal [10, 11]. Nevertheless, the usefulness of scNT is clearly diminished by its low cloning efficiency and the high levels of phenotypic variability observed in cloned animals that survive to adulthood.

Compromised umbilical cords (CUCs) are defined as malformed arteries that exhibit an artery-artery diameter difference of approximately 50% [12]. Very recently, we reported that scNT clones with CUCs (scNT-CUCs) are closely associated with poor perinatal outcome, including stillbirth and early death after birth [12]. Despite its importance in development and the need for a basic understanding of umbilical cord abnormalities, the underlying mechanisms have been poorly studied. To this end, we set out to compare the expression of multiple genes in scNT clones with and without umbilical cord abnormalities. The microarray-based genomic survey is a high-throughput approach that allows parallel study of the expression patterns of thousands of genes [13]. In the present study, we discovered previously unknown gene expression patterns related to CUCs. In agreement with the sites of phenotypic alterations found in scNT-CUCs, many differentially expressed genes were shared between the gene lists for comparisons between scNT-derived clones with normal umbilical cords (scNT-Ns) and scNT-CUCs, suggesting that common pathways are affected by the technique and

[1]Supported in part by BioGreen21 grants (PJ007189 and PJ007065) from the RDA, Republic of Korea.
[2]Correspondence: FAX: 82 2 458 5414;
e-mail: vanthuan@konkuk.ac.kr
[3]Correspondence: FAX: 82 2 455 1044;
e-mail: jhkim541@konkuk.ac.kr

Received: 2 May 2010.
First decision: 27 May 2010.
Accepted: 24 August 2010.

eISSN: 1529-7268 http://www.biolreprod.org
ISSN: 0006-3363

culture system used for scNT and that many of these unique genes are good candidates for screening umbilical cords with compromised arteries.

MATERIALS AND METHODS

Ethics Statement

The treatment of the pigs used in this research followed the guidelines of the National Institute of Animal Science's Institutional Animal Care and Use Committee, Suwon, South Korea (approval no. 2009-004, D-grade).

In Vitro Maturation of Oocytes

Ovaries were collected from prepubertal gilts at a local slaughterhouse and transported to the laboratory at 25–35°C. Antral follicles (diameter, 2–6 mm) were aspirated with an 18-gauge needle, and aspirated oocytes, with an evenly granulated cytoplasm and surrounded by at least three uniform layers of compact cumulus cells, were selected and washed three times in Tyrode lactate-Hepes with 0.1% polyvinyl alcohol (PVA). Oocytes were cultured in four-well plates containing North Carolina State University-23 (NCSU-23) medium (500 μl/well) supplemented with 10% porcine follicular fluid, 0.6 mmol/L of cysteine, 1 mmol/L of dibutyryl cAMP (dbcAMP; Sigma-Aldrich), and 0.1 IU/ml of human menopausal gonadotropin (hMG; Teikokuzoki) for 20 h. Oocytes were further cultured without dbcAMP and hMG for another 18–24 h as reported previously [3–6, 8, 9, 12, 14–17].

scNT and Embryo Transfer

Nuclear transfer was carried out as described in previous reports [3–6, 8, 9, 12, 14–17]. Briefly, mature eggs with the first polar body were cultured in NCSU-23 medium supplemented with 0.4 mg/ml of demecolcine (Sigma-Aldrich) and 0.05 mol/L of sucrose for 1 h. Sucrose was used to enlarge the perivitelline space of the eggs. Treated eggs with a protruding membrane were moved to medium supplemented with 5 mg/ml of cytochalasin B and 0.4 mg/ml of demecolcine, and the protrusion was removed with a beveled pipette. A single donor fetal fibroblast cell derived from a Gestational Day 30-derived Duroc, Berkshire, or three-way hybrid (Landrace × Duroc × Yorkshire) fetus was injected into the perivitelline space of each egg and electrically fused using two direct current pulses of 150 V/mm for 50 msec in 0.28 mol/L of mannitol supplemented with 0.1 mM $MgSO_4$ and 0.01% PVA (Sigma-Aldrich). Fused eggs were cultured in medium with 0.4 mg/ml of colcemid for 1 h before parthenogenetic activation and then cultured in 5 mg/ml of cytochalasin B-supplemented medium for 4 h. The reconstructed oocytes were activated by two direct current pulses of 100 V/mm for 20 msec in 0.28 mol/L of mannitol supplemented with 0.1 mmol/L of $MgSO_4$ and 0.05 mmol/L of $CaCl_2$. Activated eggs were cultured in the NCSU-23 medium for 6 days in an atmosphere of 5% CO_2 and 95% air at 39°C.

Sampling of CUCs

Gilts (Duroc × Yorkshire × Landrace; age, ≥8 mo) were used as recipients, and estrous synchronization of recipients was carried out as reported previously [3–6, 8, 9, 12, 14–17]. The scNT embryos were surgically transferred into the oviducts of synchronized recipients, and the pregnancy status of recipients was determined by ultrasound between Days 30 and 35. The recipients produced scNT-derived piglets via vaginal delivery. In total, 65 cloned pigs were obtained from 24 recipients using each donor fibroblast cell derived from a Duroc, Berkshire, or three-way hybrid (Landrace × Duroc × Yorkshire) fetus [12]. Of these, nine piglets were derived from Duroc, 12 piglets from three-way hybrid, and 44 piglets from Berkshire. Three clones with CUCs, based on the morphological changes of umbilical cords, were found in Birkshire-derived piglets (referring to scNT-CUC-205, -207, and -208). In addition, to minimize breeder variability, normal umbilical cord samples were also collected from three Berkshire-derived scNT-Ns showing the normal growth even 6 mo after birth and no phenotypical abnormalities. However, three scNT-CUCs showing malformed umbilical cords died suddenly within the first week of birth.

Generation of Pig Oligonucleotide 13K Microarray Chip

A total of 13 297 oligonucleotide probes (pig genome Array-Ready Oligo Sets, Version 1.0) were purchased from Operon Biotechnologies, Inc. [18]. These probes represent 10 665 *Sus scrofa* genes with a similarity to known human and mouse transcripts or 3′ expressed sequence tag. They were originally designed using the Institute of Genome Research Gene Index Database SsGI Release 5.0. To verify chip quality and effective normalization, we also spotted control samples in each block. In this pig oligonucleotide 13K chip, each of 24 blocks consists of 24 columns and 24 rows and contains 568 genes.

Hybridization

The microarray experiments were performed as described previously [19]. Briefly, each RNA (30 μg) from the umbilical cord of three scNT-Ns and three scNT-CUCs was labeled with Cy3- and Cy5-conjugated dCTP (GE Healthcare) during reverse transcription reaction using a reverse transcriptase, SuperScript II (Invitrogen). The labeled cDNAs were mixed and hybridized simultaneously to the pig oligonucleotide 13K chip. To control the gene-specific dye bias, we performed a dye-swap experiment for all samples as described previously [20]. Processed slides were scanned using an Axon 4000B Scanner (Axon Instruments), with excitation at 532 and 635 nm for the Cy3 and Cy5 dyes, respectively. The scanned images for each slide were analyzed using the GenPix Pro 5.1 Software (Axon Instruments).

Microarray Data Processing and Analysis

Microarray data were managed with GeneSpring 7.2 software (Silliconge-netics). The raw intensity data were normalized by intensity-dependent normalization in Lowess method [21] and then again by with-print-tip group normalization method for each print-tip. A total of 48 tips were used for making this pig oligonucleotide 13K chip. S-plus PLUS software (TIBCO Software) was used to determine the means of data from triplicate experiments. The gene expression values for each array were normalized to their respective median values. All clustering analyses were performed using standard correlations as described previously [22, 23]. Fold-change filters included the requirement that the genes should be expressed in umbilical cords of scNT-CUCs at least 2-fold higher or lower than in those of scNT-N controls.

RNA Isolation and Real-Time RT-PCR

Total RNA was extracted from umbilical cord tissue using a Micro-to-Midi Total RNA Purification System (Life Technologies, Inc.). Real-time RT-PCR was conducted using a DNA Engine OPTICON2 system (MJ Research) and SYBR Green as the double-stranded DNA-specific fluorescent dye (SYBR Green qPCR premix; Finnzymes). Target gene expression levels were normalized to *GAPDH* gene expression, which was unaffected in scNT-derived pigs. The RT-PCR primer sets are shown in Table 1. Real-time RT-PCR was performed independently in triplicate for different samples, and the data are presented as the mean value of gene expression measured in each individual scNT-N and scNT-CUC sample, which is used as an experimental unit.

Western Blot Analysis

Western blot analysis was performed as described previously [5, 12]. Molecular weight standards were obtained from New England Biolabs. Membranes were probed with primary antibodies recognizing *SOD2* (gifts from Dr. Han Geuk Seo, GyeongSang National University, Jinju, South Korea); *JUNB*, *JUN*, *FOSL2*, *YWHAE*, *PRDX2*, *BAX*, *BAD*, and *CYCS* antibodies were purchased from Santa Cruz Biotechnology. Active *CASP3* was from Merck & Co., and the *ACTB* antibody was from Chemicon. Thereafter, the membranes were incubated with an appropriate horseradish peroxidase-conjugated secondary antibody (Jackson Immunoresearch) and subjected to enhanced chemiluminescence (ECL) analysis (Amersham). An anti-actin antibody (1:500; Chemicon) was used to verify equal protein loading, and signals were visualized using the ECL kit (Amersham). Band intensities representing the expression of each protein were quantified by Image processing and analyzed using Image J 1.23 (NIH Image).

Statistics

Values are reported as the mean ± standard deviation. Ratios of fetal weight to placental weight in Figure 1B were analyzed using 10 scNT-N and nine scNT-CUC samples. Analysis of relative expression of genes in Figure 3 was performed using three scNT-N and three scNT-CUC umbilical cords. Statistical significances was confirmed using *t*-test.

RESULTS

Cloned scNT-Derived Piglets Exhibit CUCs

Previously, we reported that 9 of 65 scNT clones showed CUCs and compromised umbilical veins, presenting with gross

TABLE 1. Primer sets used in this study.

Gene	Description	Primer[a]	Length (bp)	GenBank accession no.
JUN	JUN family, proto-oncogene	F: CCCAAGATCCTGAAGCAGAG R: GATGTGCCCGTTACTGGACT	174	NM_213880
JUNB	JUN family, proto-oncogene	F: ACCATCAGCTACCTCCCACA R: TTCTCGGCCTTGAGTGTCTT	287	CB470397
JUND	JUN family, proto-oncogene	F: CCATCGACATGGACACTCAG R: GGACCTTCTGCTTGAGTTGC	207	DN126116
FOS	FOS family, proto-oncogene	F: AGAATCCGAAGGGAAAGGAA R: CTTCTCCTTCAGCAGGTTGG	150	AJ132510
FOSB	FOS family, proto-oncogene	F: GCCAGGAACCAGTTACTCCA R: GCGAACCCTTCTCTTCTCCT	187	AF120155
FOSL1	FOS-like antigen 1	F: GGAGCGAGTGAGTCAGAACC R: CACTCACAGCGTTGATGCTT	189	BP149434
FOSL2	FOS-like antigen 2	F: TATCCCGGGAACTTTGACAC R: CATGGAGGTGATCACTGTGG	204	BX923668
GAPDH	Glyceraldehyde-3-phosphate dehydrogenase	F: AAGTGGACATTGTCGCCATC R: TCACAAACATGGGGGCATC	318	X94251

[a] F, forward; R, reverse.

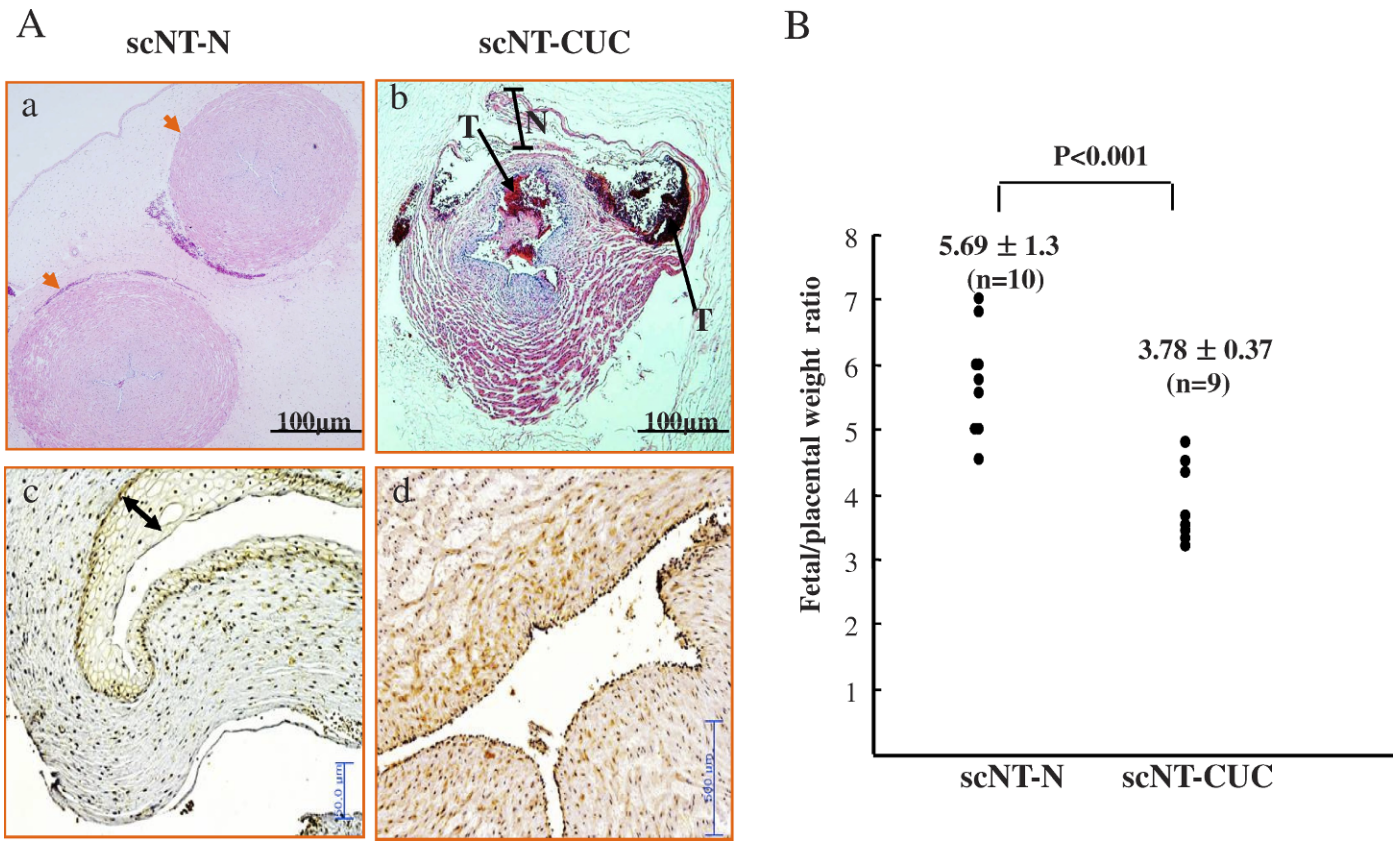

FIG. 1. Photomicrographs of cross-sections from scNT-N- and scNT-CUC-derived pig term umbilical cords. **A**) Dewaxed paraffin sections were stained with hematoxylin and eosin. Under the microscope, scNT-N-derived umbilical cord showed normal arteries (**a**), but scNT-CUC-derived umbilical cord (**b**) showed complete occlusion, resulting from a fresh thrombosis, in one umbilical artery and necrosis of the inner arterial wall with thrombosis. N, necrotic arterial wall; T, thrombosis. In the allantoic duct, scNT-N (**c**) showed columnar epithelium, but scNT-CUC lacked the epithelial layer (**d**). Original magnification ×200 (**a** and **c**) and ×400 (**b** and **d**); bars = 100 μm (**a** and **b**), 50 μm (**c**), and 500 μm (**d**). **B**) Ratio of fetal weight to placental weight in scNT-Ns and scNT-CUCs. The ratios of scNT-CUCs were significantly lower than those of the scNT-Ns. (Here, scNT-N and scNT-CUC indicate scNT clones with normal umbilical cords that survived to adulthood and scNT clones with CUC, respectively.)

necrosis and thrombosis, respectively [12]. In the present study, microscopic analyses of the nine scNT-CUCs revealed complete occlusive thrombi in the umbilical arteries (Fig. 1Ab) that were not detected in the umbilical arteries (Fig. 1Aa) of scNT-Ns. Moreover, whereas the allantoic ducts of the scNT-Ns exhibited columnar epithelium (Fig. 1Ac, arrow), the scNT-CUCs lacked this epithelial layer (Fig. 1Ad).

Next, the relationship between postnatal death and survival to adulthood were compared, and the associated factors were analyzed. The fetal weight:placental weight ratios ($n = 9$; 3.78 ± 0.37) of scNT-CUCs were significantly lower than those of the scNT-Ns ($n = 10$; 5.69 ± 1.3) (Fig. 1B). In general, scNT clones survived to adulthood when the fetal weight:placental weight ratio exceeded five, whereas a ratio of less than five showed significant association with postnatal early death among scNT clones. This observation may partly explain the high mortality rates of scNT-CUCs soon after birth [12].

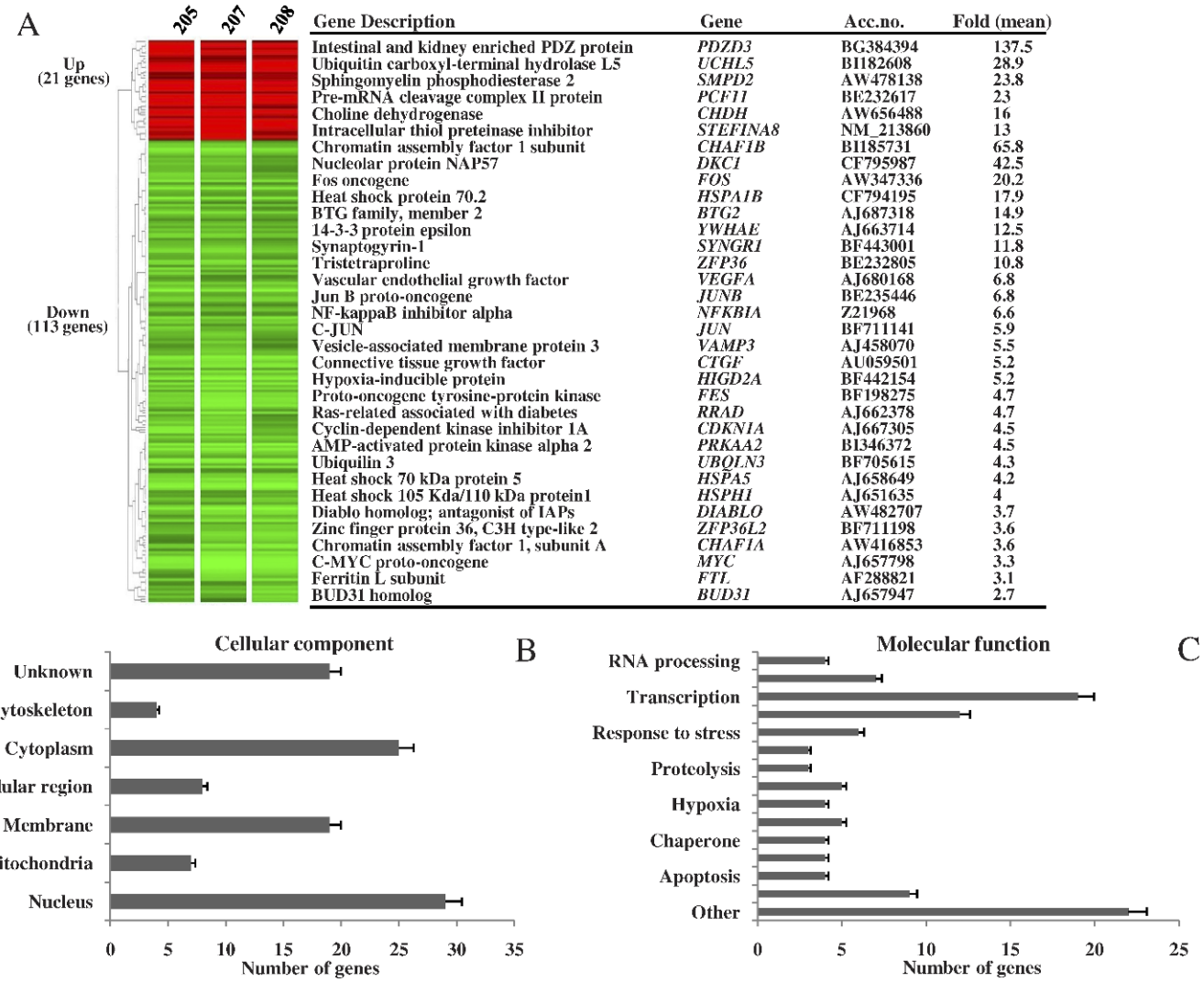

Gene Description	Gene	Acc.no.	Fold (mean)
Intestinal and kidney enriched PDZ protein	*PDZD3*	BG384394	137.5
Ubiquitin carboxyl-terminal hydrolase L5	*UCHL5*	BI182608	28.9
Sphingomyelin phosphodiesterase 2	*SMPD2*	AW478138	23.8
Pre-mRNA cleavage complex II protein	*PCF11*	BE232617	23
Choline dehydrogenase	*CHDH*	AW656488	16
Intracellular thiol preteinase inhibitor	*STEFINA8*	NM_213860	13
Chromatin assembly factor 1 subunit	*CHAF1B*	BI185731	65.8
Nucleolar protein NAP57	*DKC1*	CF795987	42.5
Fos oncogene	*FOS*	AW347336	20.2
Heat shock protein 70.2	*HSPA1B*	CF794195	17.9
BTG family, member 2	*BTG2*	AJ687318	14.9
14-3-3 protein epsilon	*YWHAE*	AJ663714	12.5
Synaptogyrin-1	*SYNGR1*	BF443001	11.8
Tristetraproline	*ZFP36*	BE232805	10.8
Vascular endothelial growth factor	*VEGFA*	AJ680168	6.8
Jun B proto-oncogene	*JUNB*	BE235446	6.8
NF-kappaB inhibitor alpha	*NFKBIA*	Z21968	6.6
C-JUN	*JUN*	BF711141	5.9
Vesicle-associated membrane protein 3	*VAMP3*	AJ458070	5.5
Connective tissue growth factor	*CTGF*	AU059501	5.2
Hypoxia-inducible protein	*HIGD2A*	BF442154	5.2
Proto-oncogene tyrosine-protein kinase	*FES*	BF198275	4.7
Ras-related associated with diabetes	*RRAD*	AJ662378	4.7
Cyclin-dependent kinase inhibitor 1A	*CDKN1A*	AJ667305	4.5
AMP-activated protein kinase alpha 2	*PRKAA2*	BI346372	4.5
Ubiquilin 3	*UBQLN3*	BF705615	4.3
Heat shock 70 kDa protein 5	*HSPA5*	AJ658649	4.2
Heat shock 105 Kda/110 kDa protein1	*HSPH1*	AJ651635	4
Diablo homolog; antagonist of IAPs	*DIABLO*	AW482707	3.7
Zinc finger protein 36, C3H type-like 2	*ZFP36L2*	BF711198	3.6
Chromatin assembly factor 1, subunit A	*CHAF1A*	AW416853	3.6
C-MYC proto-oncogene	*MYC*	AJ657798	3.3
Ferritin L subunit	*FTL*	AF288821	3.1
BUD31 homolog	*BUD31*	AJ657947	2.7

FIG. 2. Microarray analysis of scNT-CUCs and scNT-Ns. Cy5-labeled cDNAs from individual scNT-CUCs (205, 207, 208) were independently mixed with pooled Cy3-labeled cDNAs from three scNT-Ns to minimize the variation between the scNT-N control groups. The analysis of genes expressed more than 2-fold above or below the median fold-value in umbilical cords from scNT-CUCs (205, 207, and 208) compared to scNT-Ns is shown. **A**) Colors indicate the relative expression levels of each gene, with red indicating the highest expression above the median value and green indicating the lowest expression below the median value. The 134 differentially down-regulated genes were organized according to cellular component (**B**) and molecular function (**C**).

To assess differentially expressed genes of the CUC in more detail, gene expression profiles of scNT-CUC-205, -207, and -208 were analyzed using Pig 13K oligonucleotide microarrays.The results showed that 134 genes were differentially expressed with a more than 2-fold change in expression. Of note, most of the differentially expressed genes in scNT-CUCs were down-regulated (113 genes), with only 21 genes showing up-regulation. These up-regulated genes included cytoskeleton-related gene (*B2M*), proteolysis-related gene (*UCHL5*, *UBE2V2*, and *STEFIN A8*), transcription-related gene (*CDK9* and *C14orf166*), transport-related gene (*IAG2*), and others (*PDZD3*, *PCF11*, *RASGRP1*, *ARGLU1*, *C8G*, *NELL2*, *LOC68117*, *KARS*, *CD163*, *PCK2*, *LOC283951*, *SMPD2*, *CHDH*, and *PPP6C*) (Table 2).

Classification and Characterization of Identified Genes

The 134 unique genes identified with high confidence were classified in terms of molecular function and biological process using the Panther classification system. Panther is a software program freely accessible on the Web (www.pantherdb.org) that provides a platform for assigning families, functional classifications, and pathways to gene products [24, 25]. The results, expressed as pie charts using the Panther classification system, are shown in Figure 2, B and C. In the classification based on biological process (cellular component in Fig. 2B), proteins categorized as ''nucleus proteins'' were the most abundant and accounted for 32.4% of the total number of genes identified. In the classification based on molecular function, the categories containing most genes were ''transcription'' (13.6%), ''signal transduction'' (11.1%), and ''angiogenesis'' (8.5%) (Fig. 2C).

Differential DNA Expression in scNT-CUCs

Differentially expressed genes were identified using fold-change analysis of pairwise comparisons between groups of abnormal scNT-CUC and scNT-N samples. Of all the differentially expressed genes, 113 genes were down-regulated in all scNT-CUCs when compared to scNT-Ns and their fold-

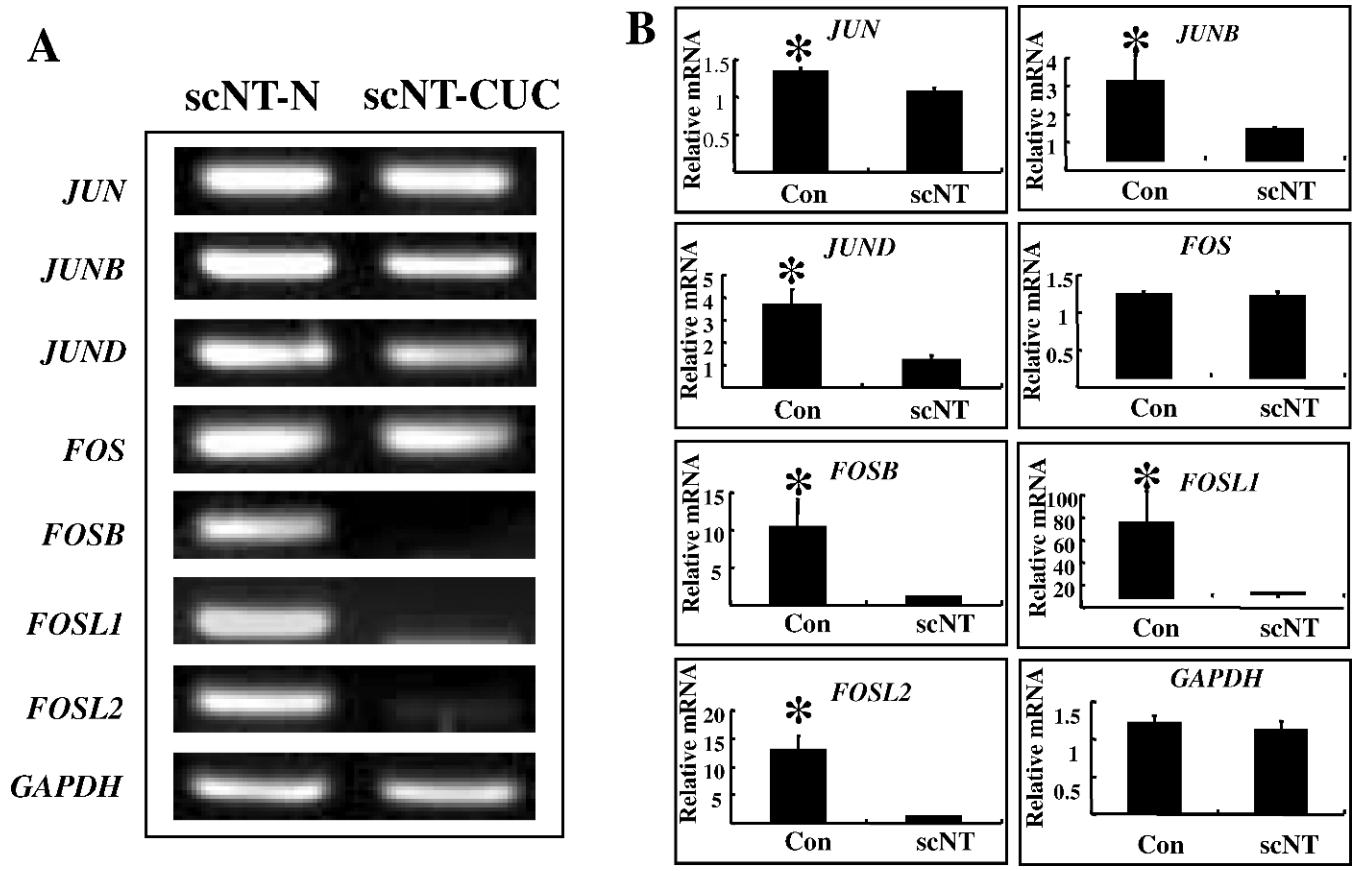

FIG. 3. Relative expression of down-regulated genes in scNT-CUC-derived term pig umbilical cords (205, 207, and 208) compared to scNT-N term pig umbilical cords. **A**) Electrophoretic analysis of real-time RT-PCR reactions in scNT-CUC and scNT-N term pig umbilical cords. **B**) Quantification of real-time RT-PCR analysis in scNT-CUC and scNT-N term pig umbilical cords. All RT-PCR reactions were conducted in triplicate and normalized for *GAPDH* mRNA expression. Each of these relative values was further divided by that of the calibrator (control), and relative expression is presented as an n-fold expression difference, compared to the calibrator. *, $P < 0.05$.

TABLE 2. Differential up-regulated genes in SCNT-derived umbilical cord with CUC.

No.	Functional role	Gene	Description	ScNT205/N[a]	ScNT207/N[a]	ScNT208/N[a]	GenBank accession no.
1	Cytoskeleton	*B2M*	Beta 2-microglobulin	3.73	3.49	5.60	AJ666710
2	Proteolysis	*UCHL5*	Ubiquitin carboxyl-terminal hydrolase L5	11.67	58.56	16.50	BI182608
3		*UBE2V2*	Ubiquitin-conjugating enzyme E2 variant 2	2.85	11.77	3.11	AJ654078
4	Proteolysis inhibitor	*STEFINA8*	Intracellular thiol proteinase inhibitor	8.33	17.55	14.27	NM_213860
5	Transcription	*CDK9*	Cyclin-dependent kinase 9	5.78	3.53	4.39	AJ659364
6		*C14orf166*	Similar to transcrtiptional activator	2.95	2.44	3.74	AJ301251
7	Transport	*IAG2*	Implantation-associated protein	3.13	3.62	2.05	AJ655592
8	Other	*PDZD3*	Intestinal and kidney enriched PDZ protein	127.05	71.00	214.66	BG384394
9		*PCF11*	Pre-mRNA cleavage complex II protein Pcf11	17.39	36.34	15.49	BE232617
10		*RASGRP1*	RAS guanyl releasing protein 1	11.04	9.09	14.54	AW347060
11		*ARGLU1*	Hypothetical protein FLJ10154	7.18	8.67	7.32	AJ654245
12		*C8G*	Complement component 8, gamma polypeptide	5.03	4.92	9.22	CF177604
13		*NELL2*	NEL-like 2 (chicken)	7.06	6.80	5.02	AJ684120
14		*LOC68117*	Hypothetical protein LOC68117	3.74	10.65	3.31	AJ658284
15		*KARS*	Lysyl-tRNA synthetase	3.67	10.56	3.06	AJ662979
16		*CD163*	Putative CD163 antigen	3.12	3.61	4.13	AJ661366
17		*PCK2*	Phospho enolpyruvate carboxykinase 2	2.95	4.85	2.65	AW437086
18		*LOC283951*	Hypothetical protein LOC283951	2.29	3.06	3.18	AJ659046
19		*SMPD2*	Sphingomyelin phosphodiesterase 2	24.28	28.62	18.76	AW478138
20		*CHDH*	Choline dehydrogenase	10.36	23.23	14.87	AW656488
21		*PPP6C*	Serine/threonine protein phosphatase 6	4.35	3.05	2.75	AJ664527

[a] N indicates scNT clones with normal umbilical cord.

change. GenBank accession numbers and annotations are listed in Table 3. Genes are classified into 15 groups based on function: 1) angiogenesis-related genes (*SERPINE1*, *VEGFA*, *CYR61*, *CTGF*, *TNFRSF12A*, *RHOH6*, *TNR12*, *RHOB*, *PLVAP*, and *CRIM1*), 2) apoptosis-related genes (*PHLDA2*, *DIABLO*, *PPP1R15A,* and *NFKBIA*), 3) cell cycle-related genes (*CDKN1A*, *HEATR7A*, *C13orf15*, and *PPP1CB*), 4) chaperone-related genes (*HSPA1B*, *CCT3*, *HSPH1*, and *AHSP*),

TABLE 3. Differential down-regulated genes in SCNT-derived umbilical cord with CUC.

No.	Functional role	Gene	Description	ScNT205/N[a]	ScNT207/N[a]	ScNT208/N[a]	GenBank accession no.
1	Angiogenesis	*SERPINE1*	Plasminogen activator inhibitor I	−4.55	−9.09	−10.00	Y11347
2		*VEGFA*	Vascular endothelial growth factor	−5.88	−6.67	−8.33	AJ680168
3		*CYR61*	Cysteine-rich, angiogenic inducer, 61	−6.25	−6.67	−4.55	CF789514
4		*CTGF*	Connective tissue growth factor	−5.00	−4.35	−6.67	AU059501
5		*TNFRSF12A*	FGF-inducible 14	−2.08	−2.56	−2.44	AW307982
6		*RHOH6*	Oncogene RHO H6	−2.38	−2.13	−2.04	CF788035
7		*TNR12*	Tumor necrosis factor receptor superfamily, member 12A	−2.08	−2.56	−2.44	AW307982
8		*RHOB*	Ras homolog gene family, member B	−2.38	−2.38	−2.08	CF788035
9		*PLVAP*	Plasmalemma vesicle associated protein	−2.33	−2.78	−2.22	AW480470
10		*CRIM1*	Cysteine-rich motor neuron 1	−2.44	−3.85	−3.57	AJ682975
11	Apoptosis	*PHLDA2*	Pleckstrin homology-like domain, family A, member 2	−3.57	−5.88	−3.85	BF710604
12		*DIABLO*	Diablo homolog, mitochondrial precursor	−3.13	−4.55	−3.45	AW482707
13		*PPP1R15A*	Protein phosphatase 1, regulatory (inhibitor) subunit 15A	−3.70	−2.38	−2.63	BE232281
14		*NFKBIA*	NF-kappaB inhibitor alpha	−3.85	−4.76	−11.11	Z21968
15	Cell cycle	*CDKN1A*	Cyclin-dependent kinase inhibitor 1A	−3.13	−5.56	−5.26	AJ667305
16		*HEATR7A*	Hypothetical protein KIAA1833	−20.00	−12.50	−25.00	AW482595
17		*C13orf15*	RGC32	−4.00	−5.88	−2.94	BF710843
18		*PPP1CB*	Protein phosphatase 1 beta isoform	−6.25	−6.67	−4.17	AJ657655
19	Chaperone	*HSPA1B*	Heat shock protein 70.2	−12.50	−14.29	−20.00	CF794195
20		*CCT3*	T-complex protein 1, gamma subunit	−4.17	−7.69	−2.70	AA056890
21		*HSPH1*	Heat shock 105kDa/110kDa protein 1	−5.00	−3.57	−3.70	AJ651635
22		*AHSP*	Alpha-hemoglobin stabilizing protein	−3.23	−2.04	−2.33	AW312426
23	Cytoskeleton	*DCTN1*	Dynactin 1	−4.17	−3.85	−2.94	AW416324
24		*DCTN4*	Dynactin 4	−9.09	−6.67	−10.00	AW786704
25		*KRT7*	Keratin, type II cytoskeletal 7	−2.63	−2.00	−6.25	BE014263
26		*MARK4*	MAP/microtubule affinity-regulating kinase 4	−3.70	−3.85	−2.56	BI404039
27		*INPP5K*	Skeletal muscle and kidney enriched inositol phosphatase	−2.44	−2.17	−2.50	BE031813
28	Hypoxia	*PLAUR*	Urokinase plasminogen activator surface receptor precursor	−12.50	−3.85	−2.17	AJ662390
29		*YWHAE*	14-3-3 protein epsilon	−11.4	−9.5	−16.6	AJ663714
30		*DUSP1*	Dual specificity phosphatase 1	−7.69	−4.17	−5.88	CF789575
31		*ALAS2*	Delta-aminolevulinate synthase	−50.00	−16.67	−4.17	AW311979
32		*HIGD2A*	Hypoxia-inducible protein	−5.88	−4.76	−5.26	BF442154
33	Modification	*MPI*	Mannose phosphate isomerase isoform	−5.00	−3.13	−4.76	BI344019
34		*ALG3*	Asparagine-linked glycosylation 3 homolog	−2.22	−8.33	−5.26	AJ747191
35		*GALNT5*	Polypeptide N-acetylgalactosaminyltransferase 5	−3.85	−3.70	−2.94	BE235257
36		*FES*	Proto-oncogene tyrosine-protein kinase	−4.76	−5.26	−4.17	BF198275
37		*NAA10*	N-terminal acetyltransferase 10	−5.26	−5.88	−3.13	CF795375
38	Proteolysis	*UBQLN3*	Ubiquilin 3	−5.00	−4.00	−3.57	BF705615
39		*FBXO9*	F-box protein 9	−50.00	−50.00	−100.00	AJ653675
40		*CAPN10*	Calpain 10	−3.33	−4.35	−6.25	AW431144
41	Redox	*ACOX1*	Acyl-coenzyme A oxidase 1, peroxisomal	−2.00	−4.00	−3.45	AJ458129
42		*FTL*	Ferritin L subunit	−3.03	−3.85	−2.70	AF288821
43		*CPT1A*	Carnitine palmitoyl transferase I liver isoform	−20.00	−7.14	−4.17	AJ653251
44	Response to stress	*RAD23B*	UV excision repair protein RAD23 homolog B	−3.57	−5.00	−2.78	AJ653687
45		*RAD23A*	UV excision repair protein RAD23 homolog A	−5.56	−6.25	−3.85	CF795930
46		*MPG*	N-methylpurine-DNA glycosylase	−5.88	−7.14	−4.55	AW415859
47		*HSPA5*	78 kDa glucose-regulated protein	−4.76	−5.26	−2.56	AJ658649
48		*GADD45B*	Growth arrest and DNA-damage-inducible, beta	−7.14	−7.69	−5.26	AU296595
49		*CTGF*	Connective tissue growth factor	−5.00	−4.35	−6.67	AU059501
50	Signal pathway	*SMAD4*	MAD, mothers against decapentaplegic homolog 4	−6.67	−25.00	−25.00	BI119052
51		*FIBP*	Acidic fibroblast growth factor intracellular binding protein	−3.57	−3.85	−3.13	AW314067
52		*ADM*	Adrenomedullin	−4.17	−6.67	−4.76	AJ657707
53		*RPTOR*	Regulatory associated protein of mTOR	−5.26	−5.26	−4.55	BF193029
54		*RRAD*	GTP-binding protein RAD	−5.26	−5.26	−3.57	AJ662378
55		*PRKAA2*	5′-AMP-activated protein kinase, catalytic alpha-2 chain	−2.13	−5.00	−6.67	BI346372
56		*RGS3*	Regulator of G-protein signalling 3	−4.55	−3.57	−5.26	AW437050
57		*RND3*	Rho related protein Rnd3/Rho8	−4.17	−3.85	−3.23	AW436135
58		*ADORA3*	Adenosine A3 receptor	−3.45	−4.35	−3.03	AW353794
59		*RGS2*	Regulator of G-protein signaling 2	−3.03	−3.33	−2.78	AJ680312
60		*RANGAP1*	Ran GTPase activating protein 1	−2.78	−2.94	−2.94	AW315950
61		*RAP1GDS1*	RAP1, GTP-GDP dissociation stimulator 1	−2.78	−14.29	−9.09	BP434428
62	Transcription	*HBP1*	HMG-box transcription factor 1	−2.70	−4.00	−3.45	AJ661062
63		*NCOR1*	Nuclear receptor co-repressor 1	−3.13	−2.70	−3.23	AW486746
64		*BTG1*	B-cell translocation gene 1	−2.94	−3.13	−2.17	AJ661677
65		*ZMIZ1*	Retinoic acid induced 17	−25.00	−16.67	−14.29	AW785080

TABLE 3. *Continued.*

No.	Functional role	Gene	Description	ScNT205/N[a]	ScNT207/N[a]	ScNT208/N[a]	GenBank accession no.
66		*RCAN3*	Down syndrome critical region gene 1-like 2	−6.25	−12.50	−11.11	AU296044
67		*CHAF1B*	Chromatin assembly factor 1 subunit B	−100.00	−50.00	−100.00	BI185731
68		*CHAF1A*	Chromatin assembly factor 1, subunit A (p150)	−3.85	−3.45	−3.57	AW416853
69		*FOS*	Proto-oncogene protein c-fos	−12.50	−12.50	−33.33	AW347336
70		*JUNB*	Jun B proto-oncogene	−7.69	−5.00	−8.33	BE235446
71		*JUN*	Transcription factor AP-1	−4.35	−2.17	−11.11	BF711141
72		*JUND*	Jun D proto-oncogene	−3.23	−4.55	−3.70	AU296478
73		*ZSCAN21*	Zinc finger and SCAN domain containing 21	−12.50	−5.88	−6.67	AJ651960
74		*NAB2*	NGFI-A binding protein 2	−5.26	−7.14	−6.25	AW786554
75		*ZFP36L2*	Butyrate response factor 2	−3.03	−5.00	−2.86	BF711198
76		*BUD31*	BUD31 homolog	−3.03	−2.70	−2.56	AJ657947
77		*ZFP36*	Zinc finger protein 36, C3H type	−7.69	−14.29	−10.00	BE232805
78		*MYC*	C-myc proto-oncogene	−2.94	−3.45	−3.45	AJ657798
79		*BTG2*	BTG family, member 2	−7.14	−25.00	−12.50	AJ687318
80		*KLF10*	TGFB inducible early growth response	−2.70	−2.70	−2.78	AJ667081
81	Transport	*TPCN2*	Two-pore calcium channel protein 2	−2.56	−2.08	−2.86	AJ665988
82		*ABCA9*	ATP-binding cassette transporter sub-family A number 9	−2.17	−2.70	−3.23	AU055637
83		*ATP6V1H*	54 kDa vacuolar H(+)-ATPase subunit	−2.63	−4.00	−2.94	AW358934
84		*ABCC10*	ATP-binding cassette member 10	−5.88	−6.25	−8.33	AU296192
85		*COX10*	Heme A:farnesyltransferase	−9.09	−12.50	−6.67	AW480555
86		*PEX5*	Peroxisomal targeting signal receptor 1	−3.70	−4.35	−4.55	AW347015
87	RNA processing	*PNPT1*	polyribonucleotide nucleotidyltransferase 1	−3.23	−2.94	−2.94	BE014291
88		*PAPD4*	PAP associated domain containing 4	−33.33	−50.00	−50.00	BF712139
89		*DKC1*	Dyskeratosis congenita 1, dyskerin	−14.29	−100.00	−50.00	AJ665156
90		*SRSF1*	Splicing factor, arginine/serine-rich 1	−10.00	−100.00	−14.29	CF795987
91	Others	*LOC396596*	Beta-lactoglobulin	−2.44	−3.03	−2.08	BI185321
92		*ATPIF1*	ATPase inhibitory factor 1	−3.13	−2.56	−2.33	BI118929
93		*BRD2*	Bromodomain containing 2	−2.00	−3.45	−4.00	AJ301280
94		*SDS*	L-serine dehydratase	−2.44	−2.08	−2.08	AJ458094
95		*TM4SF4*	Transmembrane 4 superfamily member 4	−100.00	−50.00	−50.00	AW358790
96		*HPS4*	Hermansky-Pudlak syndrome 4	−2.38	−3.57	−2.08	BG732355
97		*SLC25A39*	Mitochondrial carrier protein CGI-69	−3.57	−2.78	−3.45	AJ685440
98		*CRYAB*	Alpha crystallin B chain	−5.00	−5.56	−6.67	AW344843
99		*NFKBIL2*	I-kappa-B-related protein	−7.14	−33.33	−14.29	AJ604870
100		*GGCT*	Gamma-glutamylcyclotransferase	−14.29	−33.33	−25.00	AW483129
101		*GLCCI1*	Glucocorticoid induced transcript 1	−12.50	−100.00	−50.00	BG733581
102		*SYNGR1*	Synaptogyrin-1	−20.00	−7.14	−8.33	BE030372
103		*S100A2*	S100 calcium binding protein A2	−2.44	−8.33	−9.09	BF443001
104		*VAMP3*	Vesicle-associated membrane protein 3	−3.57	−9.09	−4.35	BI401598
105		*MOBK1B*	Mps one binder kinase activator-like 1B	−5.00	−3.23	−8.33	AJ458070
106		*ESYT1*	Extended synaptotagmin-like protein	−2.08	−8.33	−3.70	BF191940
107		*PDXK*	Pyridoxal kinase	−3.70	−4.17	−5.56	AJ658953
108		*FAM129B*	Family with sequence similarity 129, member B	−2.63	−3.13	−5.56	AF041255
109		*SCHIP1*	Schwannomin interacting protein 1	−4.00	−4.17	−2.94	BF191807
110		*C10orf58*	Chromosome 10 open reading frame 58	−0.80	−4.55	−2.04	AW342127
111		*MPDZ*	Multiple PDZ domain protein	−2.94	−3.23	−2.63	CF791706
112		*TEX264*	Testis expressed 264	−2.86	−3.45	−2.44	AJ667457
113		*ZFAND2A*	Zinc finger, AN1-type domain 2A	−2.17	−2.33	−2.04	BX675756 AW312329

[a] N indicates scNT clones with normal umbilical cord.

5) cytoskeleton-related genes (*DCTN1*, *DCTN4*, *KRT7*, *MARK4*, and *INPP5K*), 6) hypoxia-related genes (*PLAUR*, *DUSP1*, *ALAS2*, and *HIGD2A*), 7) protein modification-related genes (*MPI*, *ALG3*, *GALNT5*, *FES*, and *NAA10*), 8) proteolysis-related genes (*UBQLN3*, *FBXO9*, and *CAPN10*), 9) redox-related genes (*YWHAE*, *ACOX1*, *FTL*, and *CPT1A*), 10) stress-related genes ([*RAD23B*, *RAD23A*, *MPG*, *HSPA4*, *GADD45B*, and *CTGF*), 11) signal pathway-related genes (*SMAD4*, *FIBP*, *ADM*, *RPTOR*, *RRAD*, *PRKAA2*, *RGS3*, *RND3*, *ADORA3*, *RGS2*, *RANGAP1*, and *RAP1GDS1*), 12) transcription-related genes (*HBP1*, *NCOR1*, *BTG1*, *ZMIZ1*, *RCAN3*, *CHAF1B*, *CHAF1A*, *FOS*, *JUNB*, *JUN*, *JUND*, *ZSCAN21*, *NAB2*, *ZFP36L2*, *BUD31*, *ZFP36*, *MYC*, *BTG2*, and *KLF10*), 13) transport-related genes (*TPCN2*, *ABCA9*, *ATP6V1H*, *ABCC10*, *COX10*, and *PEX5*), 14) RNA processing-related genes (*PNPT1*, *PAPD4*, *DKC1*, and *SRSF1*), and 15) others (*LOC396596*, *ATPIF1*, *BRD2*, *SDS*, *TM4SF4*, *HPS4*, *SLC25A39*, *CRYAB*, *NFKBIL2*, *GGCT*, *GLCCI1*, *SYNGR1*, *S100A2*, *VAMP3*, *MOBK1B*, *ESYT1*, *PDXK*, *FAM129B*, *SCHIP1*, *C10orf58*, *MPDZ*, *TEX264*, and *ZFAND2A*).

Down-Regulation of JUN, JUNB, *and* FOSL2 *Cause a Ripple Effect that Alters Receptor Tyrosine Kinase Signaling*

In our DNA chip study, the most important finding was that most molecules (*JUN*, *JUNB*, *JUND*, *FOS*, *FOSB*, *FOSL1*, and *FOSL2*) involved in receptor tyrosine kinase (RTK) signaling, including vascular endothelial growth factor (*VEGF*), showed lower expression in scNT-CUC samples than in scNT-N samples (Table 3). To illustrate the reliability of the microarray data and to validate the findings, we conducted quantitative real-time RT-PCR on umbilical cord total RNA from scNT-N

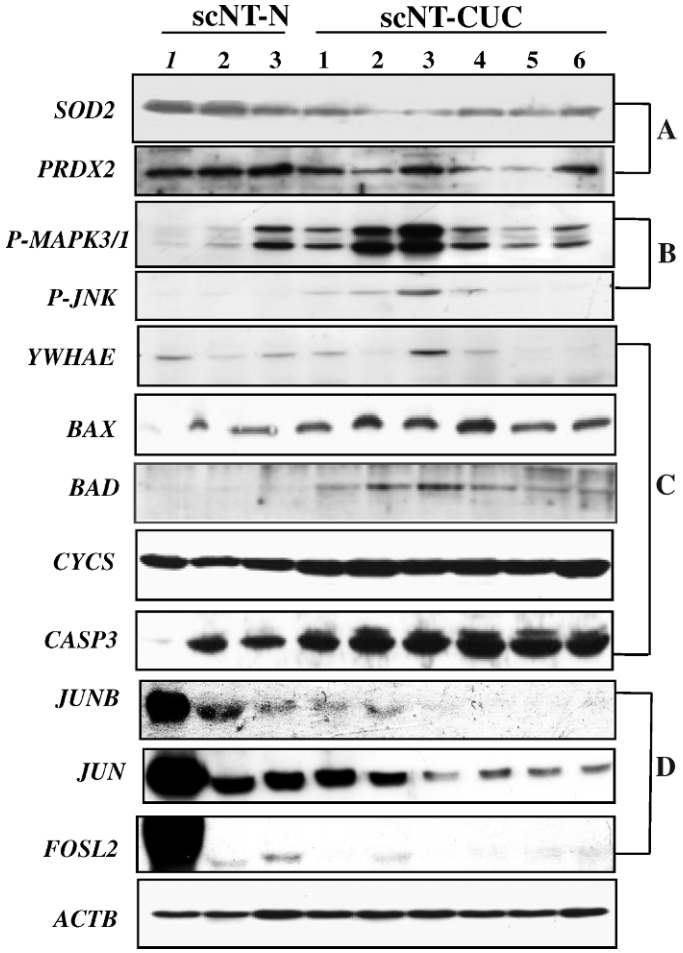

FIG. 4. Validation of microchip data by Western blot analysis. Western blot analyses were performed on samples from normal (n = 3) and hypoplastic (n = 6) scNT-derived umbilical cords. Representative analyses of antioxidant (**A**), RTK signaling (**B**), apoptosis (**C**), and transcription factors (**D**) are shown. *ACTB* was used as a control. Although antioxidant proteins and transcription factors are significantly down-regulated, RTK signaling- and apoptosis-regulated protein expression was significantly up-regulated in scNT-CUC-derived umbilical cords compared to the controls. Data represent three independent experiments.

and scNT-CUC samples for seven chosen genes (*JUN*, *JUNB*, *JUND*, *FOS*, *FOSB*, *FOSL1*, and *FOSL2*) (Fig. 3). In addition, we evaluated protein expression in scNT-N and scNT-CUC samples for three genes, *JUN*, *JUNB*, and *FOSL2*, which are involved in the regulation of transcription (Fig. 4D). All seven genes and three proteins showed the same trend with respect to changes between scNT-N and scNT-CUC samples when analyzed by real-time RT-PCR and microarray. Quality-control measures, including the ratios of the housekeeping genes glyceraldehyde-3-phosphate dehydrogenase (*GAPDH*) and *ACTB*, scaling factors, background, and *Q*-values were all within acceptable limits. Taken together, our findings show that the CUC is associated with relatively low expression of RTK signaling molecules.

Low Antioxidant Gene Expression Related to Dysfunction of scNT-Derived Umbilical Cord

Previously, we reported that scNT-derived umbilical cords with thrombosis showed extensive apoptosis [12]. Apoptosis can be triggered by many different cellular stimuli, including various types of stress and damage, and consists of a cascade of events leading to the ordered dismantling of critical cell survival components and pathways. As shown in Tables 2 and 3, we found that apoptosis-related genes (*UCHL5* and *CDK9*) were up-regulated but that antioxidation-related genes (*YWHAE*, *DUSP1*, *ALAS2*, and *HIGD2A*) and stress-related genes (*RAD23A*, *RAD23B*, *MPG*, *HSPA5*, *GADD45B*, and *CTGF*) were significantly down-regulated.

The 14-3-3 protein family members have been implicated in the protection of cells from apoptosis through binding to the pro-apoptotic protein BAD [5, 26]. Therefore, we next examined expression of the *YWHAE* gene, which was among the 113 genes that were down-regulated in scNT-CUC samples (Table 3). Although *YWHAE* gene expression was high in all scNT-N samples, most scNT-CUC samples exhibited significantly lower expression of this gene (12.5-fold). To determine the effect of *YWHAE* protein down-regulation on apoptosis, we performed Western blot analysis of scNT-N and scNT-CUC samples. It is interesting to note that Western blot analysis demonstrated that *BAX*, *CYCS*, and *CASP3* protein expression in scNT-CUC samples showed a significant increase when compared to scNT-N samples (Fig. 4C), suggesting that apoptosis in scNT-CUCs occurred following the down-regulation of antioxidants, such as *SOD2*, *PRDX2*, and *YWHAE*. Considering that the umbilical cord plays a role in the transportation of metabolites to the fetus, placental insufficiency in scNT-CUCs may be caused by an increase in apoptotic protein expression from scNT-derived umbilical cords with hypoplastic arteries. Taken together, our results provide evidence that porcine oligonucleotide microarray analysis is a useful tool for screening for scNT-derived abnormalities in pigs.

DISCUSSION

The umbilical cord normally contains one vein and two arteries [27]. Many intrapartum complications and adverse perinatal outcomes, including stillbirth and intrauterine growth restriction, have been associated with umbilical cord abnormalities. At present, the classification of these malformations is based on angiographic, intraoperative, and histological findings [28–33]. Therefore, the scNT-CUC piglet is a good model for the study of reduced cloning efficiency.

Signal Transduction

Previously, we reported that 9 of 65 scNT cloned pigs exhibited a CUC [12], and the present study extends our proteomic analysis to create a transcriptional profile for the mechanism underlying umbilical cord abnormalities in scNT clones. As far as we are aware, no study has been conducted with the purpose of elucidating a specific association between CUC and mRNA expression patterns. As shown in Figure 4, B and C, in scNT-CUCs the expression of two signal transduction-related genes, extracellular signal-regulated kinase (*ERK*) 1/2 and c-Jun N-terminal kinase (*JNK*), was significantly down-regulated. At nontoxic levels, H_2O_2 acts as a mediator of signal transduction in various cellular systems via the mitogen-activated protein kinase (*MAPK*) pathway [34, 35]. *MAPK* is a family of serine/threonine-specific protein kinases, consisting of three isoforms: *MAPK1/3* (*ERK 1/2*), *MAPK14* (*p38 MAPK*), and *MAPK8* (*JNK*) [36, 37]. On the other hand, high levels of H_2O_2 are toxic to cells and cause the oxidation of biological macromolecules, resulting in DNA breaks, lipid peroxidation, and oxidative damage of proteins. This is referred to as oxidative stress, and it is associated with the vascular apoptosis mediated by *JNK* [38–40].

In the present study, scNT-CUC samples showed relatively low expression of JUNB, JUN, and FOSL2 proteins involved in RTK signaling (Figs. 3 and 4D) [4]. In general, the RTK signaling pathway is involved in a wide range of fundamental cellular processes, including the cell cycle, cell migration, proliferation, and differentiation [41]. In a mouse model, *JUNB*$^{-/-}$ fetuses die between Embryonic Days 8.5 and 10.0 because of multiple defects in extraembryonic tissues, such as the placental labyrinth [42]. In addition, c-Fos participates in cell differentiation, growth, and transport processes that occur in mouse extraembryonic tissues [43]. Taken together, the presence of abnormal umbilical cords in scNT clones suggests that a failure in the fetomaternal exchange of nutrients, resulting from defects in umbilical cord tissues, may be the ultimate cause of the low efficiency in scNT cloning. Moreover, the results reported here provide the first evidence, to our knowledge, that members of the AP-1 transcription factor complex, such as *JUNB*, *JUN*, and *FOSL2*, play a key role in umbilical cord development.

Metabolism

Oxidative stress involves the physiological modulation of cells, tissues, and lipids as a result of their interactions with free radicals. These interactions can increase, decrease, or alter the function of specific proteins, depending upon the degree and type of protein modulation. Free radicals are highly unstable molecules that interact quickly and aggressively with other molecules in our bodies to create abnormal cells [44]. They are capable of penetrating and damaging the DNA of a cell to produce mutations that cause the cell to replicate out of control. In the present study, stress-related genes (*RAD23A*, *RAD23B*, *MPG*, *HSPA5*, *GADD45B*, and *CTGF*) and antioxidant enzymes, such as *SOD2* and *PRDX2* (Fig. 4A), were down-regulated significantly. *SOD2* and *PRDX2* are well-known proteins that protect the cell against oxidative stress. This reduction in protein expression could be a result of the inability of the cell to protect itself against oxidative stress, which suggests that down-regulation of these genes can disrupt endothelial cell function in the umbilical cord.

Angiogenesis

CYR61 is an estrogen-regulated gene that promotes cell adhesion, migration, and neovascularization [45–47]. Previous studies have demonstrated that hypoxia-inducible factor-1 alpha (*HIF1A*) interacts with *JUN* and may thereby contribute to the transcriptional regulation of *CYR61* under hypoxic conditions in human melanoma cells [46]. In the present study, we found that the angiogenesis-related genes (*SERPINE1*, *VEGFA*, *CYR61*, *CTGF*, *TNFRSF12A*, *RHOH6*, *TNR12*, *RHOB*, *PLVAP*, and *CRIM1*) in scNT umbilical cords with hypoplastic arteries were significantly down-regulated (Table 3). Thus, a reduction in the number of cells expressing *CYR61* mRNA may be caused by the down-regulation of other angiogenesis-related genes, resulting in the development of an umbilical cord with compromised arteries. However, the specific mechanisms through which *CYR61* mediates the pathogenesis of the umbilical cord remain to be fully elucidated.

A strong inducer of vascular permeability, *VEGF* is also a stimulator of endothelial cell migration and proliferation and an important factor in the survival of newly formed blood vessels [48–50]. In the present study, most of the angiogenesis-related genes were significantly down-regulated (Table 3). Furthermore, adrenomedullin (*AM*) and *VEGF* gene expression was significantly down-regulated in compromised scNT-derived umbilical cords. In cultured endothelial cells, *AM* and *VEGF* act together to induce angiogenic effects in vitro [51, 52]. The angiogenic actions of *AM*, however, appear to be independent of *VEGF* secretion [53], suggesting that *AM* is not influenced by the up-regulation of *VEGF*.

A recent study, however, suggested that *AM*-mediated signals can interact with *VEGF*-mediated signaling pathways and that *AM* plays a key role in development of the vascular system, because *AM* homozygous knockout mice (*AM*$^{-/-}$) died in utero as a result of poor angiogenesis in the placenta [54]. Therefore, the down-regulation of *AM* and *VEGF* in endothelial cells from compromised scNT-derived umbilical cords would mean that *AM* and *VEGF* could not promote cell proliferation and differentiation into cord-like structures. In fact, our previous data showed that scNT-CUC-derived endothelial cells migrated and formed tubules more slowly than control and scNT-N-derived cells [12]. Furthermore, endothelial cells in scNT-CUC samples could not elicit mitogenic responses and induce tubule formation as a result of the down-regulation of the vascular signaling molecules, *VEGF*, angiopoietin, and/or their cognate receptors, which play essential roles in vascular development. Collectively, our studies clearly demonstrate that scNT-CUCs show impaired endothelial cell migration and angiogenesis, which could lead to the development of CUC and/or placental insufficiency.

Apoptosis

The 14-3-3 proteins block *BAD*-mediated cell death by promoting the accumulation of *BAD* (phosphorylated at Ser-155), rendering it incapable of binding to *BCL2L1* [5, 55, 56]. Interestingly, our results showed that *BAD* expression increased in scNT-CUCs, whereas expression of its counterparts, the 14-3-3 proteins, decreased. Moreover, we also observed a marked increase in the expression of apoptotic signal-related proteins, such as *CYCS* and *CASP3*, in scNT-CUCs. As mentioned above, the causative mechanism for CUC is poorly understood, but these results suggest that it may entail an apoptosis-related signal transduction pathway, involving up-regulated, proapoptotic *BAD* activity and down-regulated 14-3-3 expression.

Recently, we reported that increased oxygen demand during CUC development leads to an increased rate of production for reactive oxygen species (ROS): Oxidative stress contributes to ROS formation in the CUC, and ROS levels increase gradually during early pregnancy, resulting in apoptotic cell death in CUCs [12]. In the present study, the expression of most detoxification-related proteins and antioxidant enzymes, particularly *SOD2*, was down-regulated in scNT-CUCs (Fig. 4A). Therefore, our data suggest that disruption of the antioxidant defense system and subsequent apoptotic cell death is another characteristic feature of scNT-CUCs.

In conclusion, in the present study, gene expression profiling of CUCs derived from scNT clones was performed to examine why scNT-derived clones often exhibit malformed umbilical arteries. Compared to scNT-Ns, scNT-CUCs exhibited severe histological damage, including tissue swelling and vein and arterial damage with complete occlusive thrombi. Moreover, scNT-CUCs showed a significant decrease in the expression of genes involved in transcriptional regulation, such as *JUN*, *JUNB*, and *FOSL2*, which may produce a ripple effect capable of altering the transcriptomes of many other cellular processes, including angiogenesis, antioxidation, and apoptosis. In fact, scNT-CUCs with thrombosis showed extensive apoptosis leading to placental insufficiency and its related

pathology. Even though conflicting data from Affymetrix chips and quantitative RT-PCR are found and could be a result of cross-hybridization and probe location [57, 58], the results of the present study, like those of other studies, showed a strong correlation between microarray data and quantitative RT-PCR measurements, promoting confidence in the quantitative nature of microarray data. In addition, our findings confirm the correlation between histopathological data and gene expression levels in scNT piglets, providing the evidence that porcine oligonucleotide microarray analysis is a useful tool for screening scNT-derived abnormalities in pigs.

ACKNOWLEDGMENT

We thank Dr. Patrick Hughes (Bioedit) for assistance with preparation of the manuscript.

REFERENCES

1. Arnold DR, Bordignon V, Lefebvre R, Murphy BD, Smith LC. Somatic cell nuclear transfer alters peri-implantation trophoblast differentiation in bovine embryos. Reproduction 2006; 132:79–90.
2. Hiendleder S, Mund C, Reichenbach HD, Wenigerkind H, Brem G, Zakhartchenko V, Lyko F, Wolf E. Tissue-specific elevated genomic cytosine methylation levels are associated with an overgrowth phenotype of bovine fetuses derived by in vitro techniques. Biol Reprod 2004; 71: 217–223.
3. Chae JI, Cho SK, Seo JW, Yoon TS, Lee KS, Kim JH, Lee KK, Han YM, Yu KJ. Proteomic analysis of the extraembryonic tissue from cloned porcine embryos. Mol Cell Proteomics 2006; 5:1559–1566.
4. Chae JI, Yu K, Cho SK, Kim JH, Koo DB, Lee KK, Han YM. Aberrant expression of developmentally important signaling molecules in cloned porcine extraembryonic tissues. Proteomics 2008; 8:2724–2734.
5. Lee SY, Park JY, Choi YJ, Cho SK, Ahn JD, Kwon DN, Hwang KC, Paik SS, Seo HG, Lee HT, Kim JH. Comparative proteomic analysis associated with term placental insufficiency in cloned pig. Proteomics 2007; 8:1303–1315.
6. Hill JR, Roussel AJ, Cibelli JB, Edwards JF, Hooper NL, Miller MW, Thompson JL, Looney CR, Westhusin ME, Robl JM, Stice SL. Clinical and pathologic features of cloned transgenic calves and fetuses (13 case studies). Theriogenology 1999; 51:1451–1465.
7. Cibelli JB, Campbell KH, Seidel GE, West MD, Lanza RP. The health profile of cloned animals. Nat Biotechnol 2002; 20:13–14.
8. Park MR, Cho SK, Park JY, Lee SY, Choi YJ, Kwon DN, Son WJ, Seo HG, Kim JH. Detection of rare Leydig cell hypoplasia in somatic cell cloned male piglets. Zygote 2004; 12:305–331.
9. Park MR, Cho SK, Lee SY, Choi YJ, Park JY, Kwon DN, Son WJ, Paik SS, Kim T, Han YM, Kim JH. A rare and often unrecognized cerebromeningitis and hemodynamic disorder: a major cause of sudden death in somatic cell cloned piglets. Proteomics 2005; 5:1928–1939.
10. Bondioli K, Ramsoondar J, Williams B, Costa C, Fodor W. Cloned pigs generated from cultured skin fibroblasts derived from a H-transferase transgenic boar. Mol Reprod Dev 2001; 60:189–195.
11. Lai L, Kolber-Simonds D, Park KW, Chung HT, Greenstein JL, Im GS, Samuel M, Bonk B, Rieke A, Day BN, Murphy CN, Carter DB, Hawley RJ, Prather RS. Production of alpha-1,3-galactosyltransferase knockout pigs by nuclear transfer cloning. Science 2002; 295:1089–1092.
12. Park JY, Kim JH, Choi YJ, Hwang KC, Cho SK, Park HH, Paik SS, Kim T, Park C, Lee HT, Seo HG, Park SB, et al. Comparative proteomic analysis of malformed umbilical cords from somatic cell nuclear transfer-derived piglets: implications for early postnatal death. BMC Genomics 2009; 10:511–526.
13. Konu O, Kane JK, Barrett T, Vawter MP, Chang R, Ma JZ, Donovan DM, Sharp B, Becker KG, Li MD. Region-specific transcriptional response to chronic nicotine in rat brain. Brain Res 2001; 909:194–203.
14. Yin XJ, Cho SK, Park MR, Im YJ, Park JJ, Bhak JS, Kwon DN, Jun SH, Kim NH, Kim JH. Nuclear remodeling and the developmental potential of nuclear transferred porcine oocytes under delayed-activated conditions. Zygote 2003; 11:167–174.
15. Cho SK, Kim JH, Park JY, Choi YJ, Bang JI, Hwang KC, Cho EJ, Sohn SH, Uhm SJ, Koo DB, Lee KK, Kim T, et al. Serial cloning of pigs by somatic cell nuclear transfer: restoration of phenotypic normality during serial cloning. Dev Dyn 2007; 236:3369–3382.
16. Cho SK, Hwang KC, Choi YJ, Bui HT, Nguyen VT, Park C, Kim JH, Kim JH. Production of transgenic pigs harboring the human erythropoietin (hEPO) gene using somatic cell nuclear transfer. J Reprod Dev 2009; 55: 128–136.
17. Hwang KC, Cho SK, Lee SH, Park JY, Kwon DN, Choi YJ, Park C, Kim JH, Park KK, Hwang S, Park SB, Kim JH. Depigmentation of skin and hair color in the somatic cell cloned pig. Dev Dyn 2009; 238:1701–1708.
18. Zhao SH, Recknor J, Lunney JK, Nettleton D, Kuhar D, Orley S, Tuggle CK. Validation of a first-generation long-oligonucleotide microarray for transcriptional profiling in the pig. Genomics 2005; 86:618–625.
19. Jo JH, Kim SJ, Yeon JP, Oh MJ, Seo H, Hwang SY, Kim SK, Kim BH. Effects of olanzapine on gene expression changes in MK-801-induced neurotoxicity using a high-density DNA microarray. Mol Cell Toxicol 2007; 3:282–291.
20. Yao B, Rakhade SN, Li Q, Ahmed S, Krauss R, Draghici S, Loeb JA. Accuracy of cDNA microarray methods to detect small gene expression changes induced by neuregulin on breast epithelial cells. BMC Bioinformatics 2004; 5:99.
21. Yang YH, Dudoit S, Luu P, Lin DM, Peng V, Ngai J, Speed TP. Normalization for cDNA microarray data: a robust composite method addressing single and multiple slide systematic variation. Nucleic Acids Res 2002; 30:e15.
22. Jiang D, Pei J, Zhang A. Towards interactive exploration of gene expression patterns. SIGKDD Explorations 2003; 5:79–90.
23. Park N, Katikaneni P, Skern T, Gustin KE. Differential targeting of nuclear pore complex proteins in poliovirus-infected cells. J Virol 2008; 82:1647–1655.
24. Thomas PD, Campbell MJ, Kejariwal A, Mi H, Karlak B, Daverman R, Diemer K, Muruganujan A, Narechania A. PANTHER: a library of protein families and subfamilies indexed by function. Genome Res 2003; 13: 2129–2141.
25. Mi H, Dong Q, Muruganujan A, Gaudet P, Lewis S, Thomas PD. PANTHER version 7: improved phylogenetic trees, orthologs and collaboration with the Gene Ontology Consortium. Nucleic Acids Res 2010; 38:D204–D210.
26. Datta SR, Katsov A, Hu L, Petros A, Fesik SW, Yaffe MB, Greenberg ME. 14-3-3 Proteins and survival kinases cooperate to inactivate BAD by BH3 domain phosphorylation. Mol Cell 2000; 6:41–51.
27. Belov S. Classification of congenital vascular defects. Int Angiol 1990; 9: 141–146.
28. Belov S. Anatomopathological classification of congenital vascular defects. Semin Vasc Surg 1993; 6:219–224.
29. Petrikovsky B, Schneider E. Prenatal diagnosis and clinical significance of hypoplastic umbilical artery. Prenat Diagn 1996; 16:938–940.
30. Achiron R, Hegesh J, Yagel S, Lipitz S, Cohen SB, Rotstein Z. Abnormalities of the fetal central veins and umbilico-portal system: prenatal ultrasonographic diagnosis and proposed classification. Ultrasound Obstet Gynecol 2000; 16:539–548.
31. Gamzu R, Zalel Y, Jacobson JM, Screiber L, Achiron R. Type II single umbilical artery (persistent vitelline artery) in an otherwise normal fetus. Prenat Diagn 2002; 22:1040–1043.
32. Wu JL, Fang KH, Yeh GP, Chou PH, Hsieh CT. Using color Doppler sonography to identify the perivesical umbilical arteries: a useful method in the prenatal diagnosis of omphalocele-exstrophy-imperforate anus-spinal defects complex. J Ultrasound Med 2004; 23:1211–1215.
33. Cristina MP, Ana G, Ines T, Manuel GE, Enrique IG. Perinatal results following the prenatal ultrasound diagnosis of single umbilical artery. Acta Obstet Gynecol Scand 2005; 84:1068–1074.
34. Sauer H, Wartenberg M, Hescheler J. Reactive oxygen species as intracellular messengers during cell growth and differentiation. Cell Physiol Biochem 2001; 11:173–186.
35. Touyz RM. Recent advances in intracellular signaling in hypertension. Curr Opin Nephrol Hypertens 2003; 12:165–174.
36. Miyata Y, Nishida E. Distantly related cousins of MAP kinase: biochemical properties and possible physiological functions. Biochem Biophys Res Commun 1999; 266:291–295.
37. Widmann C, Gibson S, Jarpe MB, Johnson GL. Mitogen-activated protein kinase: conservation of a three-kinase module from yeast to human. Physiol Rev 1999; 79:143–180.
38. Zalba G, Beaumont J, San Jose G, Fortuno A, Fortuno MA, Diez J. Vascular oxidant stress: molecular mechanisms and pathophysiological implications. J Physiol Biochem 2000; 56:57–64.
39. Kyriakis JM, Avruch J. Mammalian mitogen-activated protein kinase signal transduction pathways activated by stress and inflammation. Physiol Rev 2001; 81:807–869.
40. Allen RT, Krueger KD, Dhume A, Agrawal DK. Sustained Akt/PKB activation and transient attenuation of c-jun N-terminal kinase in the

inhibition of apoptosis by IGF-1 in vascular smooth muscle cells. Apoptosis 2005; 10:525–535.
41. Schlessinger J. Cell signaling by receptor tyrosine kinases. Cell 2000; 103: 211–225.
42. Schorpp-Kistner M, Wang ZQ, Angel P, Wagner EF. JunB is essential for mammalian placentation. EMBO J 1999; 18:934–948.
43. Muller R, Verma IM, Adamson ED. Expression of c-onc genes: c-fos transcripts accumulate to high levels during development of mouse placenta, yolk sac and amnion. EMBO J 1983; 2:679–684.
44. Cadet J, Douki T, Ravanat JL. Oxidatively generated base damage to cellular DNA. Free Radic Biol Med 2010; 49:9–21.
45. Brigstock DR. The CCN family: a new stimulus package. J Endocrinol 2003; 178:169–175.
46. Kunz M, Moeller S, Koczan D, Lorenz P, Wenger RH, Glocker MO, Thiesen HJ, Gross G, Ibrahim SM. Mechanisms of hypoxic gene regulation of angiogenesis factor Cyr61 in melanoma cells. J Biol Chem 2003; 278:45651–45660.
47. Gashaw I, Hastings JM, Jackson KS, Winterhager E, Fazleabas AT. Induced endometriosis in the baboon (*Papio anubis*) increases the expression of the proangiogenic factor CYR61 (CCN1) in eutopic and ectopic endometria. Biol Reprod 2006; 74:1060–1066.
48. Klagsbrun M, D'Amore PA. Vascular endothelial growth factor and its receptors. Cytokine Growth Factor Rev 1996; 7:259–270.
49. Ferrara N. Vascular endothelial growth factor: molecular and biological aspects. Curr Top Microbiol Immunol 1999; 237:1–30.
50. Neufeld G, Cohen T, Gengrinovitch S, Poltorak Z. Vascular endothelial growth factor (VEGF) and its receptors. J FASEB 1999; 13:9–22.
51. Ribatti D, Nico B, Spinazzi R, Vacca A, Nussdorfer GG. The role of adrenomedullin in angiogenesis. Peptides 2005; 26:1670–1675.
52. Ribatti D, Conconi MT, Nussdorfer GG. Nonclassic endogenous regulators of angiogenesis. Pharmacol Rev 2007; 59:185–205.
53. Guidolin D, Albertin G, Spinazzi R, Sorato E, Mascarin A, Cavallo D, Antonello M, Ribatti D. Adrenomedullin stimulates angiogenic response in cultured human vascular endothelial cells: involvement of the vascular endothelial growth factor receptor 2. Peptide 2008; 29:2013–2023.
54. Shindo T, Kurihara Y, Nishimatsu H, Moriyama N, Kakoki, Wang Y. Vascular abnormalities and elevated blood pressure in mice lacking adrenomedullin gene. Circulation 2001; 104:1964–1971.
55. Xing H, Zhang S, Weinheimer C, Kovacs A, Muslin AJ. 14-3-3 Proteins block apoptosis and differentially regulate MAPK cascades. EMBO J 2000; 19:349–358.
56. Samuel T, Weber HO, Rauch P, Verdoodt B, Eppel JT, McShea A, Hermeking H, Funk JO. The G_2/M regulator 14-3-3 sigma prevents apoptosis through sequestration of Bax. J Biol Chem 2001; 276:45201–45206.
57. Canales RD, Luo Y, Willey JC, Austermiller B, Barbacioru CC, Boysen C, Hunkapiller K, Jensen RV, Knight CR, Lee KY, Ma Y, Maqsodi B, et al. Evaluation of DNA microarray results with quantitative gene expression platforms. Nat Biotechnol 2006; 24:1115–1122.
58. Shi L, Reid LH, Jones WD, Shippy R, Warrington JA, Baker SC, Collins PJ. The MicroArray Quality Control (MAQC) project shows inter- and intraplatform reproducibility of gene expression measurements. Nat Biotechnol 2006; 24:1151–1161.